

# Accepted Manuscript

\Veratric acid derivatives containing benzylidene-hydrazine moieties as promising tyrosinase inhibitors and free radical scavengers

Zahra Dehghani, Mahsima Khoshneviszadeh, Mehdi Khoshneviszadeh, Sara Ranjbar

PII: S0968-0896(19)30406-7  
DOI: <https://doi.org/10.1016/j.bmc.2019.04.016>  
Reference: BMC 14870

To appear in: *Bioorganic & Medicinal Chemistry*

Received Date: 11 March 2019  
Revised Date: 7 April 2019  
Accepted Date: 9 April 2019

Please cite this article as: Dehghani, Z., Khoshneviszadeh, M., Khoshneviszadeh, M., Ranjbar, S., \Veratric acid derivatives containing benzylidene-hydrazine moieties as promising tyrosinase inhibitors and free radical scavengers, *Bioorganic & Medicinal Chemistry* (2019), doi: <https://doi.org/10.1016/j.bmc.2019.04.016>

This is a PDF file of an unedited manuscript that has been accepted for publication. As a service to our customers we are providing this early version of the manuscript. The manuscript will undergo copyediting, typesetting, and review of the resulting proof before it is published in its final form. Please note that during the production process errors may be discovered which could affect the content, and all legal disclaimers that apply to the journal pertain.



**Veratric acid derivatives containing benzylidene-hydrazine moieties as promising tyrosinase inhibitors and free radical scavengers**

Zahra Dehghani<sup>a,c</sup>, Mahsima Khoshneviszadeh<sup>b</sup>, Mehdi Khoshneviszadeh<sup>a,b\*</sup>, Sara Ranjbar<sup>c\*\*</sup>

*<sup>a</sup>Department of Medicinal Chemistry, School of Pharmacy, Shiraz University of Medical Sciences, Shiraz, Iran*

*<sup>b</sup>Medicinal and Natural Products Chemistry Research Center, Shiraz University of Medical Sciences, Shiraz, Iran*

*<sup>c</sup>Pharmaceutical Sciences Research Center, Shiraz University of Medical Sciences, Shiraz, Iran*

**Corresponding Authors:**

**\*Mehdi Khoshneviszadeh**

Department of Medicinal Chemistry, School of Pharmacy, Shiraz University of Medical Sciences, Shiraz, Iran

Tel: +98 713 230 3872; Fax: +98 713 230 2225; E-mail: [m.khoshneviszadeh@gmail.com](mailto:m.khoshneviszadeh@gmail.com)

**\*\*Sara Ranjbar**

Pharmaceutical Sciences Research Center, Shiraz University of Medical Sciences, Shiraz, Iran

Tel: +98 713 242 4128; Fax: +98 713 230 2225; E-mail: [ranjbar18@yahoo.com](mailto:ranjbar18@yahoo.com)  
[ranjbar90156@gmail.com](mailto:ranjbar90156@gmail.com)

**Abstract**

Tyrosinase enzyme plays a crucial role in melanin biosynthesis and enzymatic browning process of vegetables and fruits. A series of veratric acid derivatives containing benzylidene-hydrazine moieties with different substitutions were synthesized and their inhibitory effect on mushroom tyrosinase and free radical scavenging activity were evaluated. The results indicated that N'-(4-chlorobenzylidene)-3,4-dimethoxybenzohydrazide (**D5**) and N'-(2,3-dihydroxybenzylidene)-3,4-dimethoxybenzohydrazide (**D12**) showed the highest tyrosinase inhibitory activity with  $IC_{50}$  values of  $19.72 \pm 1.84$  and  $20.63 \pm 0.79$   $\mu\text{M}$ , respectively, that were comparable with the  $IC_{50}$  value of kojic acid ( $19.08 \pm 1.21$   $\mu\text{M}$ ). **D12** was also a potent radical scavenger with  $EC_{50}$  value of  $0.0097 \pm 0.0011$  mM. The free radical scavenging activity of **D12** was comparable with the standard quercetin. The inhibition kinetic analyzed by Lineweaver–Burk plots revealed that compound **D5** was a competitive tyrosinase inhibitor. Molecular docking study was carried out for the derivatives demonstrating tyrosinase inhibitory activity. **D5** and **D12** possessed the most negative estimated free energies of binding in mushroom tyrosinase active site. Therefore, **D5** and **D12** could be introduced as potent tyrosinase inhibitors that might be promising leads in medicine, cosmetics and food industry.

**Keywords:** tyrosinase inhibitor, benzohydrazide, kojic acid, diphenolase activity, veratric acid.

## 1. Introduction

Tyrosinase enzyme (EC 1.14.18.1) is a dicopper oxidase which is widely distributed in bacteria, fungi, insects, plants, and animals.<sup>1,2</sup> Tyrosinase is involved in melanin biosynthesis by catalyzing rate-limiting steps of overall melanogenesis including the hydroxylation of L-tyrosine to 3,4-dihydroxy-L-phenylalanine (L-DOPA) and subsequent oxidation of L-DOPA to dopaquinone.<sup>3,4</sup> As, tyrosinase contributes a significant role in the brain neuromelanin development and too much formation of dopaquinone leads to neuronal damage and cell death, it has been proved that the enzyme is associated to neurodegenerative disorders including Parkinson's and Huntington's diseases.<sup>5-7</sup> Moreover, tyrosinase is responsible for enzymatic browning of fruits and vegetables due to polyphenol compounds oxidation which results in quality loss and deterioration of nutritional value of fruits and vegetables during postharvest-handling and processing.<sup>8,9</sup> Therefore, inhibition of tyrosinase catalytic activity has proved to be an effective approach to treat hyperpigmentation and neurodegenerative disorders, and also to prevent food deterioration.<sup>10,11</sup> Consequently, tyrosinase inhibitors have broad applications in the fields of medicine, cosmetics, agriculture and food industry. Several compounds belonging to different classes are reported as tyrosinase inhibitors.<sup>12,13</sup> Unfortunately, these molecules have adverse side effects and low efficacy. Thus, it is of great importance to develop new, effective and non-toxic tyrosinase inhibitors.

3,4-Dimethoxybenzoic acid, known as veratric acid and derived from plants and fruits, has been reported to have some biological activities such as anti-oxidant, anti-inflammation, and blood pressure-lowering effects.<sup>14-18</sup> It has been reported that veratric acid and its methyl ester do not show significant inhibitory effect on tyrosinase.<sup>19</sup> Hydrazides, acylated derivatives of hydrazine, are a class of organic compounds containing azomethine group ( $-N=CH$ ) linked to an

amide group. Hydrazone derivatives are pharmaceutically important, as they have been reported to possess a number of biological effects such as anti-inflammatory, antitumoral, antitubercular, anticonvulsant, antioxidant, analgesic, antiplatelet, antimalarial, antimicrobial, antimycobacterial, vasodilator, antiviral and antiulcer activities.<sup>20-28</sup>

In this study, we designed veratric acid derivatives containing different benzylidene-hydrazine moieties. After the synthesis, we evaluated their tyrosinase inhibitory activity as well as their free radical scavenging effect. The most active derivative was investigated for its inhibition kinetic. Finally, molecular docking analysis was performed to gain a perception of the ligand-receptor interactions of the active derivatives.

## **2. Materials and Methods**

### **2.1. Apparatus**

Melting points were determined using a hot stage apparatus (Electrothermal, Essex, UK) and were uncorrected. Mass spectra were recorded on an Agilent spectrometer (Agilent technologies 9575c inert MSD, USA). NMR spectra were done on a Burker-Avance DPX-300 MHz in DMSO-*d*<sub>6</sub>. All spectra affirmed the structure of the synthesized compounds. Elemental analysis was performed by Microanalytical Department, Central Laboratories for Research, Shiraz University of Medical Sciences and it was within 0.4 % of the calculated value.

### **2.2. Chemicals and reagents**

All reagents and solvents were obtained from commercial suppliers and were used without further purification. Methyl 3,4-dimethoxybenzoate, hydrazine hydrate and aldehydes were purchased from Merck. Analytical thin layer chromatography (TLC) was performed on

MERCK pre-coated silica gel 60-F254 (0.5 mm) aluminum plates. Mushroom tyrosinase (EC1.14.18.1), kojic acid, dimethyl sulfoxide (DMSO), L-3,4-dihydroxyphenylalanine (L-DOPA) and 2,2-diphenyl-1-picrylhydrazyl (DPPH) were from Sigma Chemical Co. (St. Louis, MO, USA).

### 2.3. Synthesis of 3,4-dimethoxybenzohydrazide (B)

A mixture of methyl 3,4-dimethoxybenzoate (20 mmol) and hydrazine hydrate (30 mL) were refluxed in ethanol for 3 hours. The reaction proceeding was monitored by TLC. After completion of the reaction, the mixture was cooled to room temperature, the solvent was reduced and n-hexane was added to the reaction mixture. The resulted precipitate was collected and washed with cold water to give us pure 3,4-dimethoxybenzohydrazide as the intermediate (yield: 88%).

### 2.4. Synthesis of benzylidene-3,4-dimethoxybenzohydrazide derivatives (D1-D16)

A mixture of methyl 3,4-dimethoxybenzoate (1 mmol) and corresponding benzaldehyde (1 mmol) was refluxed in ethanol (7 ml) for 6 hours. Reaction completion was checked by TLC. The mixture was cooled to room temperature and the resulted precipitate was collected and washed with diethyl ether to yield the final pure products. Moreover, in some cases, recrystallization in appropriate solvents was done in order to obtain the pure derivatives.

#### 2.4.1. (*E*)-3,4-dimethoxy-*N'*-(4-nitrobenzylidene)benzohydrazide (D1)

Yellow solid; yield: 82%; M.P: 208-210 °C.  $^1\text{H}$  NMR (300 MHz, DMSO- $d_6$ ):  $\delta$  (ppm) 3.85 (s, 6H, OCH $_3$ ), 7.09 (d, 1H, Ar-H-5,  $J=6.5$  Hz), 7.42-7.58 (m, 2H, Ar-H-2, 6), 7.96 (d, 2H, Ar-H-2',6'), 8.28 (d, 2H, Ar-H-3',5'), 8.55 (s, 1H, N=CH), 12.00 (s, 1H, NH).  $^{13}\text{C}$  NMR (75

MHz, DMSO-*d*<sub>6</sub>):  $\delta$  (ppm) 56.10 (OCH<sub>3</sub>), 56.14 (OCH<sub>3</sub>), 111.46, 121.66, 121.70, 124.52, 125.53, 128.32, 141.26, 145.06, 148.20, 148.86, 152.45, 163.24 (C=O). MS (EI, 70 eV): *m/z* (%) = 329 (M<sup>+</sup>, 10), 165 (100). Anal. Calcd for C<sub>16</sub>H<sub>15</sub>N<sub>3</sub>O<sub>5</sub>: C 58.36, H 4.59, N 12.76%, found: C 58.44, H 4.61, N 12.72%.

#### 2.4.2. (*E*)-*N'*-(4-(dimethylamino)benzylidene)-3,4-dimethoxybenzohydrazide (D2)

Recrystallized in ethyl acetate. Cream solid; yield: 76%; M.P: 201-203 °C. <sup>1</sup>H NMR (300 MHz, DMSO-*d*<sub>6</sub>):  $\delta$  (ppm) 2.97 (s, 6H, NCH<sub>3</sub>), 3.83 (s, 6H, OCH<sub>3</sub>), 6.75 (d, 2H, Ar-H-3',5', *J*=7.2 Hz), 7.07 (d, 1H, Ar-H-5, *J*=7.5 Hz), 7.49-7.55 (m, 4H, Ar-H-2, 6, 2',6'), 8.33 (s, 1H, N=CH), 11.42 (s, 1H, NH). <sup>13</sup>C NMR (75 MHz, DMSO-*d*<sub>6</sub>):  $\delta$  (ppm) 40.24 (NCH<sub>3</sub>), 56.09 (OCH<sub>3</sub>), 111.33, 111.45, 112.29, 121.25, 122.22, 126.37, 128.80, 148.63, 148.81, 151.92, 152.0, 162.62 (C=O). MS (EI, 70 eV): *m/z* (%) = 327 (M<sup>+</sup>, 50), 181 (20), 165 (100), 146 (75). Anal. Calcd for C<sub>18</sub>H<sub>21</sub>N<sub>3</sub>O<sub>3</sub>: C 66.04, H 6.47, N 12.84%, found: C 66.15, H 6.46, N 12.76%.

#### 2.4.3. (*E*)-*N'*-(4-bromobenzylidene)-3,4-dimethoxybenzohydrazide (D3)

White solid; yield: 61%; M.P: 193-194 °C. <sup>1</sup>H NMR (300 MHz, DMSO-*d*<sub>6</sub>):  $\delta$  (ppm) 3.84 (s, 6H, OCH<sub>3</sub>), 7.09 (d, 1H, Ar-H-5, *J*=8.4 Hz), 7.49 (s, 1H, Ar-H-2), 7.58 (d, 1H, Ar-H-6, *J*=8.4 Hz), 7.63-7.73 (m, 4H, Ar-H-2', 3',5',6'), 8.44 (s, 1H, N=CH), 11.78 (s, 1H, NH). <sup>13</sup>C NMR (75 MHz, DMSO-*d*<sub>6</sub>):  $\delta$  (ppm) 65.142 (OCH<sub>3</sub>), 111.46, 121.51, 123.59, 125.82, 129.30, 132.30, 134.22, 146.40, 148.85, 152.29, 163.09 (C=O). MS (EI, 70 eV): *m/z* (%) = 364 ([M<sup>+</sup>+2], 6), 362 (M<sup>+</sup>, 5), 181 (33), 165 (100). Anal. Calcd for C<sub>16</sub>H<sub>15</sub>BrN<sub>2</sub>O<sub>3</sub>: C 52.91, H 4.16, N 22.00%, found: C 53.00, H 4.18, N 21.96%.

**2.4.4. (E)-N'-(3,4-dimethoxybenzylidene)-3,4-dimethoxybenzohydrazide (D4)**

White solid; yield: 79%; M.P: 198-201 °C. <sup>1</sup>H NMR (300 MHz, DMSO-*d*<sub>6</sub>): δ (ppm) 3.83 (s, 12H, OCH<sub>3</sub>), 7.02-7.09 (m, 2H, Ar-H-5, 5'), 7.19 (d, 1H, Ar-H-6', *J*=7.2 Hz), 7.34 (s, 1H, Ar-H-2'), 7.51 (s, 1H, Ar-H-6), 8.57 (d, 1H, Ar-H-2, *J*=8.1 Hz), 8.43 (s, 1H, N=CH), 11.66 (s, 1H, NH). <sup>13</sup>C NMR (75 MHz, DMSO-*d*<sub>6</sub>): δ (ppm) 55.92 (OCH<sub>3</sub>), 56.04 (OCH<sub>3</sub>), 56.12 (OCH<sub>3</sub>), 108.72, 111.39, 111.47, 112.00, 121.44, 122.20, 126.09, 127.65, 148.03, 148.80, 149.54, 151.12, 152.13, 162.94 (C=O). MS (EI, 70 eV): *m/z* (%) = 344 (M<sup>+</sup>, 17), 181 (38), 165 (100). Anal. Calcd for C<sub>18</sub>H<sub>20</sub>N<sub>2</sub>O<sub>5</sub>: C 62.78, H 5.85, N 8.13%, found: C 62.96, H 5.83, N 8.15%.

**2.4.5. (E)-N'-(4-chlorobenzylidene)-3,4-dimethoxybenzohydrazide (D5)**

White solid; yield: 66%; M.P: 186-189 °C. <sup>1</sup>H NMR (300 MHz, DMSO-*d*<sub>6</sub>): δ (ppm) 3.84 (s, 12H, OCH<sub>3</sub>), 7.08 (d, 1H, Ar-H-5, *J*=9 Hz), 7.50-7.59 (m, 4H, Ar-H-2, 6, 3', 5'), 7.75 (d, 2H, Ar-H-2', 6', *J*=8.1 Hz), 8.46 (s, 1H, N=CH), 11.78 (s, 1H, NH). <sup>13</sup>C NMR (75 MHz, DMSO-*d*<sub>6</sub>): δ (ppm) 56.10 (OCH<sub>3</sub>), 56.13 (OCH<sub>3</sub>), 111.46, 121.52, 125.84, 129.06, 129.39, 133.88, 134.82, 146.24, 146.32, 148.84, 152.30, 163.10 (C=O). MS (EI, 70 eV): *m/z* (%) = 318 (M<sup>+</sup>, 5), 181 (20), 165 (100). Anal. Calcd for C<sub>16</sub>H<sub>15</sub>ClN<sub>2</sub>O<sub>3</sub>: C 60.29, H 4.47, N 8.79%, found: C 60.36, H 4.47, N 8.81%.

**2.4.6. (E)-3,4-dimethoxy-N'-(4-methoxybenzylidene)benzohydrazide (D6)**

White solid; yield: 73%; M.P: 168-171 °C. <sup>1</sup>H NMR (300 MHz, DMSO-*d*<sub>6</sub>): δ (ppm) 3.81 (s, 3H, OCH<sub>3</sub>), 3.84 (s, 6H, OCH<sub>3</sub>), 7.01-7.09 (m, 3H, Ar-H-5, 3', 5'), 7.50-7.68 (m, 4H, Ar-H-2, 6, 2', 6'), 8.41 (s, 1H, N=CH), 11.59 (s, 1H, NH). <sup>13</sup>C NMR (75 MHz, DMSO-*d*<sub>6</sub>): δ (ppm) 55.75 (OCH<sub>3</sub>), 56.12 (OCH<sub>3</sub>), 111.38, 111.44, 114.80, 121.37, 126.11, 127.48, 129.05, 130.44,

147.64, 148.82, 152.13, 162.88 ( $\underline{\text{C}}=\text{O}$ ). MS (EI, 70 eV):  $m/z$  (%) = 314 ( $\text{M}^+$ , 14), 181 (40), 165 (100). Anal. Calcd for  $\text{C}_{17}\text{H}_{18}\text{N}_2\text{O}_4$ : C 64.96, H 5.77, N 8.91%, found: C 64.02, H 5.76, N 8.88%.

#### 2.4.7. (*E*)-3,4-dimethoxy-*N'*-(2-methoxybenzylidene)benzohydrazide (D7)

White solid; yield: 76%; M.P: 183-185 °C.  $^1\text{H}$  NMR (300 MHz,  $\text{DMSO-}d_6$ ):  $\delta$  (ppm) 3.83-3.87 (m, 9H,  $\text{OCH}_3$ ), 7.00-7.12 (m, 3H, Ar-H-5, 3', 4'), 7.41 (t, 1H, Ar-H-5',  $J=7.2$  Hz), 7.54 (s, 1H, Ar-H-2), 7.60 (dd, 1H, Ar-H-6,  $J=8.4/1.8$  Hz), 7.88 (d, 1H, Ar-H-6',  $J=7.2$  Hz), 8.83 (s, 1H,  $\text{N}=\underline{\text{CH}}$ ), 11.73 (s, 1H,  $\text{NH}$ ).  $^{13}\text{C}$  NMR (75 MHz,  $\text{DMSO-}d_6$ ):  $\delta$  (ppm) 56.10 ( $\text{OCH}_3$ ), 111.33, 111.47, 112.29, 121.20, 121.54, 122.93, 125.89, 125.93, 131.85, 143.03, 148.80, 152.18, 158.15, 162.85 ( $\underline{\text{C}}=\text{O}$ ). MS (EI, 70 eV):  $m/z$  (%) = 314 ( $\text{M}^+$ , 5), 181 (54), 165 (100). Anal. Calcd for  $\text{C}_{17}\text{H}_{18}\text{N}_2\text{O}_4$ : C 64.96, H 5.77, N 8.91%, found: C 65.15, H 5.79, N 8.94%.

#### 2.4.8. (*E*)-3,4-dimethoxy-*N'*-(3-nitrobenzylidene)benzohydrazide (D8)

Cream solid; yield: 91%; M.P: 189-192 °C.  $^1\text{H}$  NMR (300 MHz,  $\text{DMSO-}d_6$ ):  $\delta$  (ppm) 3.85 (s, 6H,  $\text{OCH}_3$ ), 7.09 (d, 1H, Ar-H-5,  $J=8.1$  Hz), 7.51 (s, 1H, Ar-H-2), 7.59 (d, 1H, Ar-H-6,  $J=7.8$  Hz), 7.75 (t, 1H, Ar-H-5',  $J=7.2$  Hz), 8.13 (d, 1H, Ar-H-4',  $J=6.0$  Hz), 8.53-8.56 (m, 2H, Ar-H-6' and  $\text{N}=\underline{\text{CH}}$ ), 11.96 (s, 1H,  $\text{NH}$ ).  $^{13}\text{C}$  NMR (75 MHz,  $\text{DMSO-}d_6$ ):  $\delta$  (ppm) 56.09 ( $\text{OCH}_3$ ), 56.14 ( $\text{OCH}_3$ ), 111.45, 121.20, 121.65, 124.55, 125.60, 130.91, 133.76, 136.80, 145.18, 148.70, 148.86, 152.40, 160.93, 163.25 ( $\underline{\text{C}}=\text{O}$ ). MS (EI, 70 eV):  $m/z$  (%) = 329 ( $\text{M}^+$ , 9), 181 (5), 165 (100). Anal. Calcd for  $\text{C}_{16}\text{H}_{15}\text{N}_3\text{O}_5$ : C 58.36, H 4.59, N 12.76%, found: C 58.49, H 4.60, N 12.71%.

**2.4.9. (E)-3,4-dimethoxy-N'-(3,4,5-trimethoxybenzylidene)benzohydrazide (D9)**

Recrystallized in chloroform-ethanol. White solid; yield: 89%; M.P: 170-173 °C. <sup>1</sup>H NMR (300 MHz, DMSO-*d*<sub>6</sub>): δ (ppm) 3.71 (s, 3H, OCH<sub>3</sub>), 3.84 (s, 12H, OCH<sub>3</sub>), 7.02 (s, 2H, Ar-H-2', 6'), 7.09 (d, 1H, Ar-H-5, *J*=8.1 Hz), 7.49 (s, 1H, Ar-H-2), 7.57 (d, 1H, Ar-H-6, *J*=7.8 Hz), 8.41 (s, 1H, N=CH), 11.71 (s, 1H, NH). <sup>13</sup>C NMR (75 MHz, DMSO-*d*<sub>6</sub>): δ (ppm) 56.09 (OCH<sub>3</sub>), 56.13 (OCH<sub>3</sub>), 56.40 (OCH<sub>3</sub>), 60.58 (OCH<sub>3</sub>), 104.67, 111.43, 111.48, 121.48, 126.00, 130.42, 139.63, 147.86, 148.82, 153.67, 163.06 (C=O). MS (EI, 70 eV): *m/z* (%) = 374 (M<sup>+</sup>, 18), 181 (33), 193 (10), 165 (100). Anal. Calcd for C<sub>19</sub>H<sub>22</sub>N<sub>2</sub>O<sub>6</sub>: C 60.95, H 5.92, N 7.48%, found: C 61.12, H 5.91, N 7.46%.

**2.4.10. (E)-N'-(4-hydroxy-3,5-dimethoxybenzylidene)-3,4-dimethoxybenzohydrazide (D10)**

Cream solid; yield: 68%; M.P: 158-161 °C. <sup>1</sup>H NMR (300 MHz, DMSO-*d*<sub>6</sub>): δ (ppm) 3.83 (s, 12H, OCH<sub>3</sub>), 6.98 (s, 2H, Ar-H-2', 6'), 7.08 (d, 1H, Ar-H-5, *J*=8.1 Hz), 7.49 (s, 1H, Ar-H-2), 7.57 (d, 1H, Ar-H-6, *J*=7.5 Hz), 8.36 (s, 1H, N=CH), 8.92 (s, 1H, OH), 11.59 (s, 1H, NH). <sup>13</sup>C NMR (75 MHz, DMSO-*d*<sub>6</sub>): δ (ppm) 55.08 (OCH<sub>3</sub>), 56.13 (OCH<sub>3</sub>), 56.49 (OCH<sub>3</sub>), 105.06, 106.28, 111.48, 121.40, 125.15, 126.17, 138.36, 148.57, 148.63, 148.82, 152.12, 162.93 (C=O). MS (EI, 70 eV): *m/z* (%) = 360 (M<sup>+</sup>, 29), 344 (12), 207 (5), 181 (41), 165 (100). Anal. Calcd for C<sub>18</sub>H<sub>20</sub>N<sub>2</sub>O<sub>6</sub>: C 59.99, H 5.59, N 7.77%, found: C 60.20, H 5.57, N 7.76%.

**2.4.11. (E)-N'-(4-hydroxybenzylidene)-3,4-dimethoxybenzohydrazide (D11)**

Cream solid; yield: 30%; M.P: 182-183 °C. <sup>1</sup>H NMR (300 MHz, DMSO-*d*<sub>6</sub>): δ (ppm) 3.84 (s, 6H, OCH<sub>3</sub>), 6.83 (d, 1H, Ar-H-5), 7.09 (d, 2H, Ar-H-3', 5'), 7.22 (d, 2H, Ar-H-2', 6'), 7.50 (s, 1H, Ar-H-2), 7.57 (d, 1H, Ar-H-6, *J*=7.8 Hz), 8.38 (s, 1H, N=CH), 9.65 (s, 1H, OH), 11.66 (s, 1H, NH). <sup>13</sup>C NMR (75 MHz, DMSO-*d*<sub>6</sub>): δ (ppm) 56.12 (OCH<sub>3</sub>), 111.46, 113.01,

117.78, 119.18, 121.46, 125.95, 130.34, 147.79, 148.84, 152.21, 158.15, 163.00 ( $\underline{\text{C}}=\text{O}$ ). MS (EI, 70 eV):  $m/z$  (%) = 300 ( $\text{M}^+$ , 9), 181 (26), 165 (100). Anal. Calcd for  $\text{C}_{16}\text{H}_{16}\text{N}_2\text{O}_4$ : C 63.99, H 5.37, N 9.33%, found: C 63.31, H 5.38, N 7.36%.

**2.4.12. (E)-N'-(2,3-dihydroxybenzylidene)-3,4-dimethoxybenzohydrazide (D12)**

Recrystallized in ethyl acetate. Cream solid; yield: 32%; M.P: 206-207 °C.  $^1\text{H}$  NMR (300 MHz,  $\text{DMSO}-d_6$ ):  $\delta$  (ppm) 3.85 (s, 6H,  $\text{OCH}_3$ ), 6.75 (t, 1H, Ar-H-5',  $J=7.2$  Hz), 6.86 (d, 1H, Ar-H-4',  $J=6.9$  Hz), 6.95 (d, 1H, Ar-H-5,  $J=6.9$  Hz), 7.11 (d, 1H, Ar-H-6',  $J=7.8$  Hz), 7.53 (s, 1H, Ar-H-2), 7.60 (d, 1H, Ar-H-6,  $J=7.5$  Hz), 8.60 (s, 1H,  $\text{N}=\underline{\text{C}}\text{H}$ ), 9.22 (s, 1H,  $\text{OH}$ ), 11.26 (s, 1H,  $\text{OH}$ ), 11.97 (s, 1H,  $\text{NH}$ ).  $^{13}\text{C}$  NMR (75 MHz,  $\text{DMSO}-d_6$ ):  $\delta$  (ppm) 56.10 ( $\text{OCH}_3$ ), 56.15 ( $\text{OCH}_3$ ), 111.38, 111.54, 117.76, 119.26, 119.60, 120.53, 121.54, 125.25, 146.06, 146.51, 148.92, 152.43, 162.72 ( $\underline{\text{C}}=\text{O}$ ). MS (EI, 70 eV):  $m/z$  (%) = 316 ( $\text{M}^+$ , 23), 181 (11), 165 (100). Anal. Calcd for  $\text{C}_{16}\text{H}_{16}\text{N}_2\text{O}_5$ : C 60.75, H 5.10, N 8.86%, found: C 60.89, H 5.09, N 8.89%.

**2.4.13. (E)-N'-(3-ethoxy-4-hydroxybenzylidene)-3,4-dimethoxybenzohydrazide (D13)**

White solid; yield: 59%; M.P: 193-196 °C.  $^1\text{H}$  NMR (300 MHz,  $\text{DMSO}-d_6$ ):  $\delta$  (ppm) 1.37 (t, 3H,  $\text{CH}_2-\underline{\text{C}}\text{H}_3$ ,  $J=6.9$  Hz), 3.83 (s, 6H,  $\text{OCH}_3$ ), 4.05-4.08 (m, 2H,  $\underline{\text{C}}\text{H}_2-\text{CH}_3$ ), 7.08 (d, 1H, Ar-H-4',  $J=8.4$  Hz), 7.24-7.30 (m, 2H, Ar-H-5, 5'), 7.44 (s, 1H, Ar-H-2'), 7.50 (s, 1H, Ar-H-2), 7.56 (d, 1H, Ar-H-6,  $J=8.4$  Hz), 8.35 (s, 1H,  $\text{OH}$ ), 8.56 (s, 1H,  $\text{N}=\underline{\text{C}}\text{H}$ ), 11.54 (s, 1H,  $\text{NH}$ ).  $^{13}\text{C}$  NMR (75 MHz,  $\text{DMSO}-d_6$ ):  $\delta$  (ppm) 15.18 ( $\text{CH}_2-\underline{\text{C}}\text{H}_3$ ), 56.08 ( $\text{OCH}_3$ ), 56.12 ( $\text{OCH}_3$ ), 64.35 ( $\underline{\text{C}}\text{H}_2-\text{CH}_3$ ), 110.81, 111.47, 111.91, 116.04, 121.37, 123.76, 125.98, 126.30, 147.60, 147.65, 149.62, 150.55, 152.10, 162.85 ( $\underline{\text{C}}=\text{O}$ ). MS (EI, 70 eV):  $m/z$  (%) = 344 ( $\text{M}^+$ , 4), 328 (100), 299 (22), 272 (37), 191 (33), 181 (8), 165 (24), 135 (19). Anal. Calcd for  $\text{C}_{18}\text{H}_{20}\text{N}_2\text{O}_5$ : C 62.78, H 5.85, N 8.13%, found: C 62.91, H 5.85, N 8.12%.

**2.4.14. (E)-N'-(3-methoxy-4-hydroxybenzylidene)-3,4-dimethoxybenzohydrazide (D14)**

White solid; yield: 53%; M.P: 171-173 °C. <sup>1</sup>H NMR (300 MHz, DMSO-*d*<sub>6</sub>): δ (ppm) 3.81-3.83 (m, 9H, OCH<sub>3</sub>), 6.96-7.09 (m, 3H, Ar-H-4', 5', 5), 7.29 (s, 1H, Ar-H-2'), 7.49 (s, 1H, Ar-H-2), 7.57 (d, 1H, Ar-H-6, *J*=7.8 Hz), 8.32 (s, 1H, OH), 9.33 (s, 1H, N=CH), 11.55 (s, 1H, NH). <sup>13</sup>C NMR (75 MHz, DMSO-*d*<sub>6</sub>): δ (ppm) 56.03 (OCH<sub>3</sub>), 56.08 (OCH<sub>3</sub>), 111.35, 111.45, 112.35, 112.73, 120.60, 121.35, 126.13, 127.77, 147.36, 147.91, 148.82, 150.16, 152.10, 162.82 (C=O). MS (EI, 70 eV): *m/z* (%) = 330 (M<sup>+</sup>, 14), 181 (39), 165 (100). Anal. Calcd for C<sub>17</sub>H<sub>18</sub>N<sub>2</sub>O<sub>5</sub>: C 61.81, H 5.49, N 8.48%, found: C 61.98, H 5.50, N 8.45%.

**2.4.15. (E)-N'-(2,4-dihydroxybenzylidene)-3,4-dimethoxybenzohydrazide (D15)**

White solid; yield: 61%; M.P: 271-273 °C. <sup>1</sup>H NMR (300 MHz, DMSO-*d*<sub>6</sub>): δ (ppm) 3.83 (s, 6H, OCH<sub>3</sub>), 6.33-6.38 (m, 2H, Ar-H-3', 5'), 7.09 (d, 1H, Ar-H-5, *J*=8.4 Hz), 7.30 (d, 1H, Ar-H-6', *J*=8.1 Hz), 7.50 (s, 1H, Ar-H-2), 7.57 (d, 1H, Ar-H-6, *J*=8.1 Hz), 8.51 (s, 1H, N=CH), 9.96 (s, 1H, OH), 11.55 (s, 1H, OH), 11.78 (s, 1H, NH). <sup>13</sup>C NMR (75 MHz, DMSO-*d*<sub>6</sub>): δ (ppm) 56.08 (OCH<sub>3</sub>), 56.12 (OCH<sub>3</sub>), 103.14, 108.11, 111.07, 111.31, 111.51, 121.39, 125.48, 131.75, 148.87, 149.16, 152.27, 159.93, 161.07, 162.46 (C=O). MS (EI, 70 eV): *m/z* (%) = 316 (M<sup>+</sup>, 9), 181 (38), 165 (100). Anal. Calcd for C<sub>16</sub>H<sub>16</sub>N<sub>2</sub>O<sub>5</sub>: C 60.75, H 5.10, N 8.86%, found: C 60.61, H 5.11, N 8.88%.

**2.4.16. (E)-4-((2-(3,4-dimethoxybenzoyl)hydrazono)methyl)-2-methoxyphenyl acetate (D16)**

White solid; yield: 33%; M.P: 114-118 °C. <sup>1</sup>H NMR (300 MHz, DMSO-*d*<sub>6</sub>): δ (ppm) 2.28 (s, 3H, O(CO)CH<sub>3</sub>), 3.84 (s, 9H, OCH<sub>3</sub>), 7.09 (d, 1H, Ar-H-5, *J*=5.4 Hz), 7.19 (d, 1H, Ar-H-5', *J*=7.2 Hz), 7.29 (d, 1H, Ar-H-6'), 7.47-7.60 (m, 3H, Ar-H-2, 6, 2'), 8.47 (s, 1H, N=CH), 11.78 (s, 1H, NH). <sup>13</sup>C NMR (75 MHz, DMSO-*d*<sub>6</sub>): δ (ppm) 20.86, 56.07 (OCH<sub>3</sub>), 56.12 (OCH<sub>3</sub>), 56.29

(OCH<sub>3</sub>), 110.75 111.46, 115.91, 120.89, 121.51, 123.77, 125.86, 133.82, 141.18, 147.14, 148.82, 151.68, 152.24, 163.11 (C=O), 168.93(O-C=O). MS (EI, 70 eV): m/z (%) = 373 (M<sup>+</sup>, 6), 330 (8), 181 (34), 165 (100). Anal. Calcd for C<sub>19</sub>H<sub>20</sub>N<sub>2</sub>O<sub>6</sub>: C 61.28, H 5.41, N 7.52%, found: C 61.30, H 5.41, N 7.54%.

## 2.5. Mushroom tyrosinase inhibition assay

Mushroom tyrosinase (EC 1.14.18.1) (Sigma Chemical Co.) was assayed using L-DOPA as the substrate as reported in our previous studies.<sup>29-31</sup> The enzyme diphenolase activity was monitored spectrophotometrically by observing dopachrome formation at 475 nm. All the test samples were first dissolved in DMSO at 40 mM and diluted to the required concentrations. Initially, 10 ml of tyrosinase (0.5 mg ml<sup>-1</sup>) was mixed with 160 ml of 50 mM phosphate buffer (pH=6.8) and then 10 ml of the test sample in 96-well microplates was added. After the mixture was pre-incubated at 28 °C for 20 min, 20 ml of L-DOPA solution (0.5 mM) was added to the phosphate buffer. DMSO without test compounds was used as the control, and kojic acid was used as a positive control. Each assay was conducted as three separate replicates. The inhibitory activity of the tested compounds was expressed as the concentration that inhibited 50% of the enzyme activity (IC<sub>50</sub>). The percentage inhibition ratio was calculated according to the following equation:

$$\text{Inhibition (\%)} = 100 (\text{Abs}_{\text{control}} - \text{Abs}_{\text{compound}}) / \text{Abs}_{\text{control}}$$

## 2.6. Determination of the inhibition type

The most potent derivative, compound **D5**, was considered for kinetic analysis. The inhibitor concentrations were: 0, 10, 25, 50 and 100 mM. Substrate (L-DOPA) concentrations were 0.25, 0.5, 0.75 and 1 mM in all kinetic studies. Pre-incubation and measurement time were the same as discussed in mushroom tyrosinase inhibition assay protocol. Maximum initial velocity was determined from initial linear portion of absorbance up to 10 min after addition of L-DOPA with 1 min interval. The Michaelis constant ( $K_m$ ) and the maximal velocity ( $V_{max}$ ) of the tyrosinase activity were determined by the Lineweaver-Burk plot at various concentrations of L-DOPA as a substrate. The inhibition type of the enzyme was assayed by Lineweaver-Burk plots of inverse of velocities ( $1/V$ ) versus inverse of substrate concentrations  $1/[S]$   $\text{mM}^{-1}$ .

## 2.7. Free radical scavenging assay

Radical scavenging activity was determined by DPPH assay. A mixture of test compounds (in different concentrations) and methanolic solution of DPPH (110  $\mu\text{M}$ ) was shaken in the dark at 37 °C for 30 min. The mixture absorbance was measured at 517 nm. Quercetin was used as the positive control. The percent scavenging activity was calculated using the following equation:

$$\text{Radical Scavenging activity (\%)} = 100 \times (\text{Abs}_{\text{control}} - \text{Abs}_{\text{compound}}) / \text{Abs}_{\text{control}}$$

The  $\text{EC}_{50}$  values were obtained from linear regression plot between concentrations of test compounds and percent radical scavenging activity. Each concentration was analyzed in three independent experiments run in triplicate.

## 2.8 Computational Details

### 2.8.1 *In silico* physicochemical parameters and pharmacokinetics calculations

The drug likeness and pharmacokinetics properties of the compounds were determined using the preADMET online server (<http://preadmet.bmdrc.org/>).

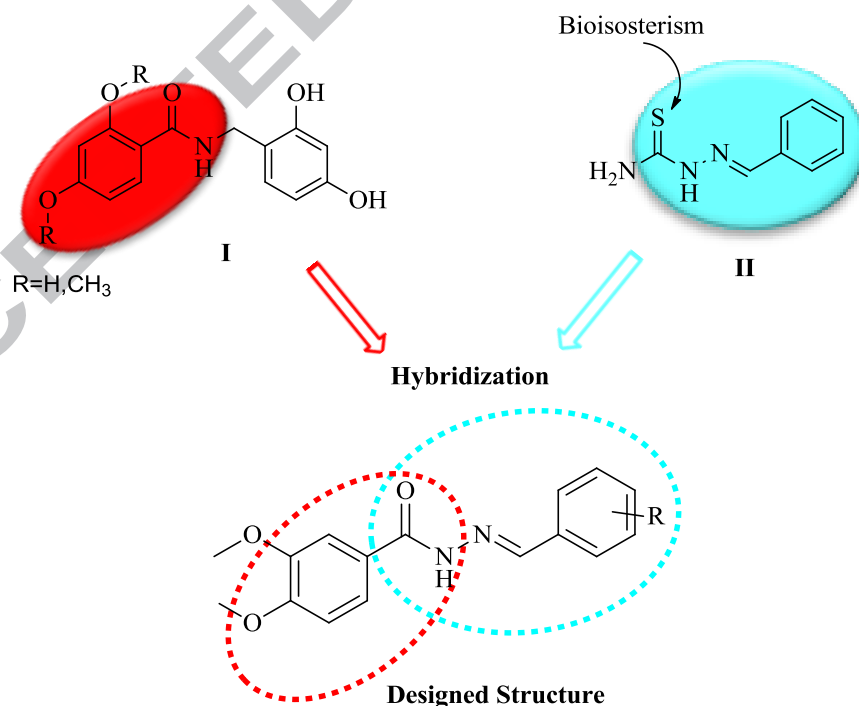
### 2.8.2 Molecular docking study

Docking was performed by AutoDock 4.2 and AutoDock Tools 1.5.4 (ADT). X-ray crystal structure of *Agaricus bisporus* tyrosinase containing tropolone as the innate ligand in the binding site (PDBID: 2Y9X) was retrieved from the RCSB Protein Databank (<http://www.rcsb.org>). Before docking, tropolone and water molecules were removed from 2Y9X. Using ADT, the crystal structure was then prepared for docking. For this purpose, hydrogens were added and non-polar hydrogens were merged and finally, Gasteiger charges were calculated for protein 2Y9X. 3-D structures of ligands were sketched and minimized under Molecular Mechanics MM+ and then Semi-empirical AM1 methods in HyperChem software. PDBQT formats of the ligands were prepared by adding Gasteiger charges and setting the degree of torsions by using ADT. The grid maps were constructed by AutoGrid and grid box dimensions were set to 40×40×40 with 0.375 Å grid spacing. The active site which comprises the amino acid residues surrounding the two copper ions was selected for docking and the grids' center were placed on the tropolone's binding site. In order to determine the docking parameter file, rigid macromolecule and Lamarckian genetic search algorithm were chosen and the number of GA runs was set at 100. Default values were retained for the rest of the parameters. Docking validity was tested using co-crystallized inhibitor as ligand and the above-mentioned procedure.

### 3. Results and discussion

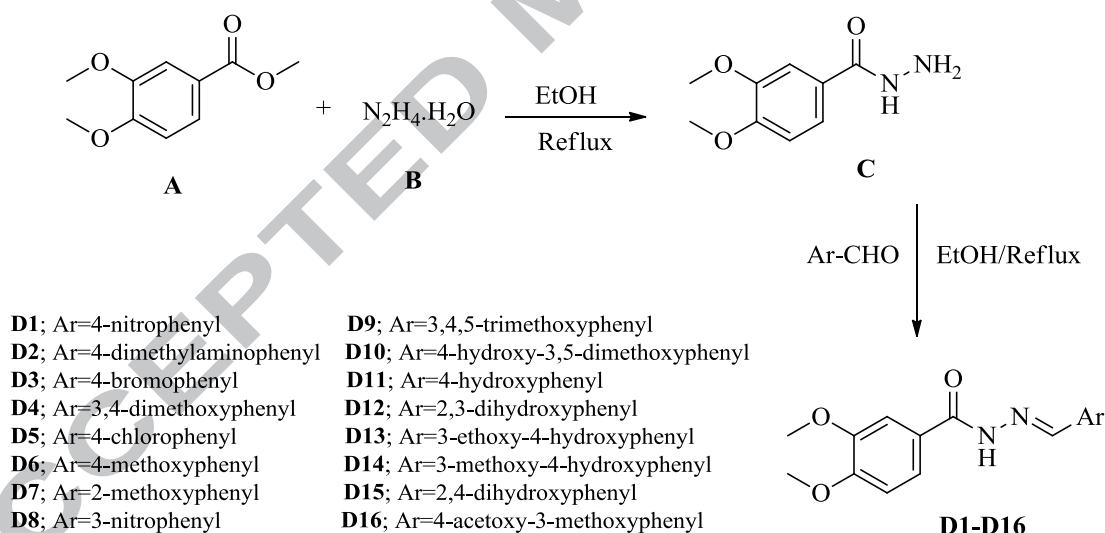
#### 3.1. Design strategy

The target N'-benzylidene-3,4-dimethoxybenzohydrazide scaffold was designed based on the structures of some potent tyrosinase inhibitors reported in the literature (**Figure 1**). Some benzamide derivatives (structure **I** in **Figure 1**) have been found to exhibit superior inhibitions on tyrosinase activity ( $IC_{50}=0.3-0.9 \mu M$ ) than kojic acid did.<sup>32</sup> Moreover, it has been reported that some hydrazine-containing compounds, such as compound **II**, were effective tyrosinase inhibitors ( $IC_{50}=1.93 \mu M$ ) which showed higher inhibitory activity than kojic acid.<sup>33</sup> Considering these structural features and principles of bioisosterism, we designed a series of benzylidene-3,4-dimethoxybenzohydrazide derivatives as tyrosinase inhibitors by applying fragment-based drug design approach. Different substituents were inserted on benzylidene moiety to define beneficial structure–activity relationships (SARs).



**Figure 1.** Fragment-based design of proposed tyrosinase inhibitors.**3.2. Synthesis**

Target compounds were synthesized *via* a two-step reaction outlined in **Scheme 1**. Initially, methyl 3,4-dimethoxybenzoate (**A**) was refluxed with hydrazine hydrate (**B**) in ethanol for 3 hours. The resultant 3,4-dimethoxybenzohydrazide (**C**) was reacted with various aryl-aldehydes (**C**) in ethanol and at reflux condition for about 6 hours to obtain final benzylidene-3,4-dimethoxybenzohydrazide derivatives (**D1-D16**). All the target compounds were synthesized in good yield and high purity. Their chemical structures were characterized and confirmed by using  $^1\text{H}$  NMR,  $^{13}\text{C}$  NMR and MS analysis.

**Scheme 1.** Synthesis of benzylidene-3,4-dimethoxybenzohydrazide derivatives (**D1-D16**).

### 3.3. Effect of N'-benzylidene-3,4-dimethoxybenzohydrazide derivatives on the diphenolase activity of mushroom tyrosinase

The inhibitory effect of the synthesized derivatives on mushroom tyrosinase activity has been evaluated and the results are presented in **Table 1**. Compounds **D7**, **D9**, **D12**, **D15** and **D16** showed good to excellent inhibition on mushroom tyrosinase with  $IC_{50}$  ranging from 19.72  $\mu$ M to 37.41  $\mu$ M, while rest of the derivatives displayed no remarkable inhibitory activity. Compounds **D5** and **D12** exhibited the highest tyrosinase inhibitory activity with  $IC_{50}$  values of  $19.72 \pm 1.84 \mu$ M and  $20.63 \pm 0.79 \mu$ M, respectively, which were comparable to that of the standard kojic acid with  $IC_{50}$  value of  $19.08 \pm 1.21 \mu$ M.

The bioassay results showed that substitutions on benzylidene played a major role in tyrosinase inhibitory activity of 3,4-dimethoxybenzohydrazid derivatives as compound **D5** bearing 4-chloro substitution exhibited excellent tyrosinase inhibitory activity ( $IC_{50}=19.72 \mu$ M). Moreover, the substitution pattern of hydroxyl and methoxy groups at phenyl ring was the decisive factor of the inhibitory activity. Considering  $IC_{50}$  values reported in **Table 1**, it could be stated that the compounds which possess hydroxyl or methoxy groups at the *ortho* and/or *meta* positions were more active than those having these substitutions at the *para* position and existence of an acetoxy group at *para* position improved the anti-tyrosinase effect. Compounds **D12** and **D16** bearing 2,3-dihydroxy and 4-acetoxy-3-methoxy residues exhibited the second and third best tyrosinase inhibitory activities ( $IC_{50}$ s=20.63 and 28.26  $\mu$ M, respectively). Replacing 3-hydroxyl with 4-hydroxyl as in **D15** ( $IC_{50}=31.53 \mu$ M), led to a considerable decrease in the activity as compared to **D12**.

**Table 1.** Antioxidant properties and tyrosinase inhibitory activities of (D1–D16).

Compound	Tyrosinase inhibitory activity <sup>a</sup>		DPPH radical scavenging activity <sup>a</sup>
	Tyrosinase inhibition <sup>b</sup>	IC <sub>50</sub> <sup>c</sup>	EC <sub>50</sub>
	(%)	( $\mu$ M)	(mM)
D1	17.68 $\pm$ 1.14	>50	>1
D2	13.60 $\pm$ 0.18	>50	0.4482 $\pm$ 0.0018
D3	19.49 $\pm$ 2.62	>50	>1
D4	13.37 $\pm$ 0.33	>50	>1
D5	69.16 $\pm$ 1.75	19.72 $\pm$ 1.84	>1
D6	28.51 $\pm$ 1.60	>50	>1
D7	59.34 $\pm$ 2.44	35.16 $\pm$ 1.08	>1
D8	15.61 $\pm$ 5.01	>50	>1
D9	57.17 $\pm$ 2.97	37.41 $\pm$ 5.22	>1
D10	25.17 $\pm$ 3.39	>50	>1
D11	22.49 $\pm$ 4.10	>50	>1
D12	69.04 $\pm$ 1.85	20.63 $\pm$ 0.79	0.0097 $\pm$ 0.0011
D13	38.33 $\pm$ 2.06	>50	0.0498 $\pm$ 0.0028
D14	39.94 $\pm$ 4.11	>50	0.4260 $\pm$ 0.0063
D15	58.70 $\pm$ 3.25	31.53 $\pm$ 2.17	0.0829 $\pm$ 0.0045
D16	60.21 $\pm$ 1.03	28.26 $\pm$ 0.94	0.1535 $\pm$ 0.0052
Kojic acid	71.74 $\pm$ 2.08	19.08 $\pm$ 1.21	-
Quercetin	-	-	0.0089 $\pm$ 0.0014

<sup>a</sup> Values represent means  $\pm$  SE of 3-4 independent experiments.

<sup>b</sup> Tyrosinase inhibition for synthesized compounds and kojic acid was measured at 50  $\mu$ M.

<sup>c</sup> 50 % inhibitory concentration (IC<sub>50</sub>).

### 3.4. Determining the inhibitory type on mushroom tyrosinase for D5 derivative

The enzyme inhibition mode by the most potent derivative, **D5**, was studied by Lineweaver–Burk plot analysis. The results are presented in **Figure 2**. Lineweaver–Burk plots (plot of  $1/V$  versus  $1/[S]$ ) for the inhibition of tyrosinase was obtained with several concentrations of **D5** (as the inhibitor) and L-DOPA (as the substrate). The plots of  $1/V$  versus  $1/[S]$  presented straight lines which crossed the y-axis at similar points. It was found that as the inhibitor concentration elevated, the value of  $K_m$  increased, but  $V_{max}$  was not affected by the concentration. Therefore, the results represented that compound **D5** is a competitive inhibitor of mushroom tyrosinase.

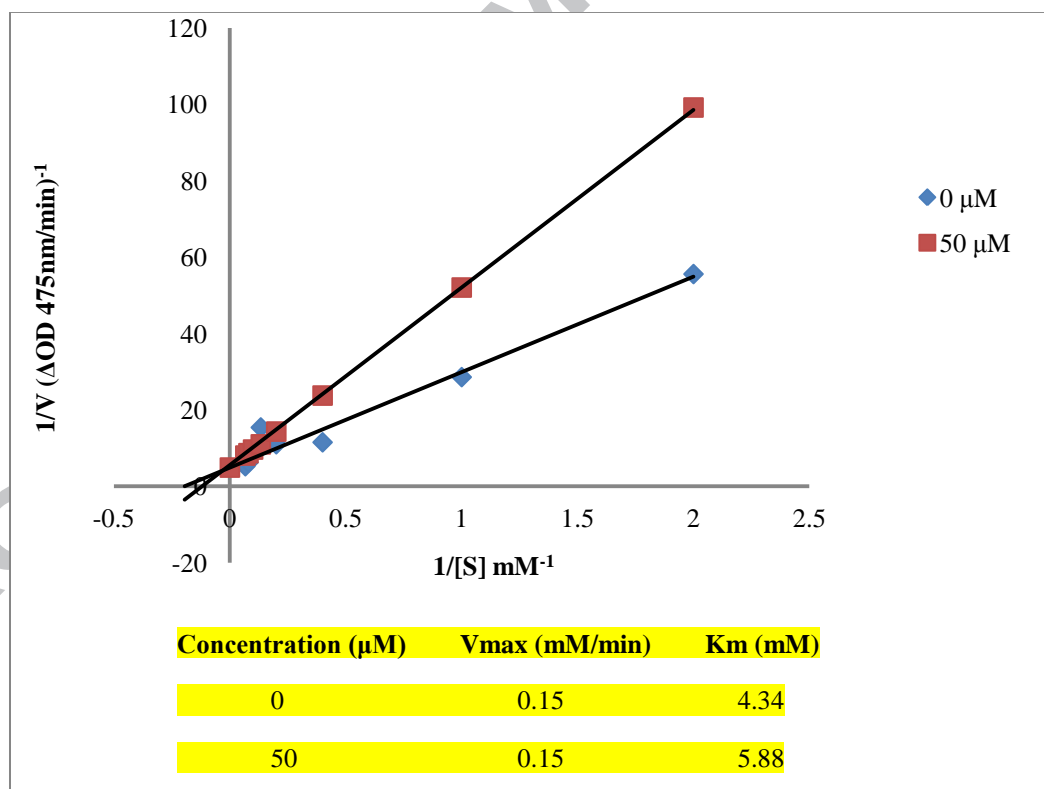


**Figure 2.** Lineweaver-Burk plot for mushroom tyrosinase enzyme inhibition by different concentrations of **D5** in the presence of L-DOPA. The reciprocal tyrosinase inhibitory activity was plotted against the reciprocal substrate concentration (double reciprocal plot,  $n = 3$ ).

### 3.5. Free radical scavenging activity

Radical scavenging of all compounds against DPPH was investigated and the  $IC_{50}$  values were determined. The results are shown in **Table 1**. Compound **D12**, having 2,3-dihydroxyphenyl substitution, exhibited the highest activity with  $EC_{50}$  value of  $0.0097 \pm 0.0011$  mM, comparable to that of quercetin as the positive control ( $EC_{50} = 0.0089 \pm 0.0014$  mM). **D13** and **D15** derivatives (bearing 3-ethoxy-4-hydroxyphenyl and 2,4-dihydroxyphenyl substituents) were found to be effective radical scavengers with  $EC_{50}$  values of  $0.0498 \pm 0.0028$  and  $0.0829 \pm 0.0045$  mM, respectively. Compounds **D2**, **D14** and **D16**, possessing 4-dimethylaminophenyl, 3-methoxy-4-hydroxyphenyl and 4-acetoxy-3-methoxyphenyl moieties, respectively, demonstrated lower radical scavenging activities with  $EC_{50}$  values ranging from 0.1535 mM to 0.4482 mM.

### 3.6. Computational section

#### 3.6.1. Drug-likeness and ADME properties

The drug likeness scores (including; Lipinski rule of five, CMC like rule, lead like rule, MDDR like rule, and WDI like rule) and pharmacokinetics properties (including; human intestinal absorption, *in vitro* Caco-2 (Caucasian colon adenocarcinoma) cell permeability, *in vitro* MDCK (Maden Darby Canine Kidney) cell permeability, *in vitro* plasma protein binding and *in vivo* BBB penetration) were predicted for the derivatives that showed tyrosinase

inhibition. Calculations were carried out using the web-based application PreADMET and the results obtained for compounds demonstrating tyrosinase inhibition are summarized in **Table 2** and **Table 3**. The data revealed that all molecules fulfill the Lipinski's rule of five, CMC like rule, MDDR like rule, and WDI like rule (**Table 2**). As it is reported in **Table 3**, all the derivatives show well intestinal absorption. The compounds are predicted to bind weakly to plasma proteins. Moreover, low blood–brain barrier permeation is observed for all the inhibitors (except **D15**), therefore, it can be stated that they are less likely to cause neurotoxicity.

Therefore, benzylidene-3,4-dimethoxybenzohydrazide tyrosinase inhibitors could serve as suitable drug-like candidates and according to ADME properties of the derivatives, they can be proposed as effective candidates for further drug development.

**Table 2.** *In silico* Lipinski rule of five, lead like rule, CMC like rule, MDDR like rule, and WDI like rule prediction for veratric acid derivatives possessing tyrosinase inhibitory activity..

<b>Code</b>	<b>CMC like rule</b>	<b>Lead like rule</b>	<b>MDDR like rule</b>	<b>Lipinski' s rule of five</b>	<b>WDI like rule</b>
<b>D5</b>	Qualified	Violated	Mid-structure	Suitable	In 90% cutoff
<b>D7</b>	Qualified	Suitable	Mid-structure	Suitable	In 90% cutoff
<b>D9</b>	Qualified	Violated	Mid-structure	Suitable	In 90% cutoff
<b>D12</b>	Qualified	Suitable	Mid-structure	Suitable	In 90% cutoff
<b>D15</b>	Qualified	Suitable	Mid-structure	Suitable	In 90% cutoff
<b>D16</b>	Qualified	Violated	Mid-structure	Suitable	In 90% cutoff

**Table 3.** *In silico* ADME profiling of veratric acid derivatives possessing tyrosinase inhibitory activity.

Code	Absorption				Distribution	
	Human intestinal	<i>In vitro</i> caco-2 cell	<i>In vitro</i> MDCK Cell	<i>In vitro</i> skin	<i>In vitro</i> plasma	<i>In vivo</i> blood–brain
	Absorption HIA (percentage)	permeability (nm s <sup>-1</sup> )	Permeability (nm s <sup>-1</sup> )	permeability (log <i>K</i> <sub>p</sub> , cm h <sup>-1</sup> )	protein binding (percentage)	barrier penetration (C.brain/C.blood)
<b>D5</b>	95.75	30.66	3.94	-2.97	88.20	0.22
<b>D7</b>	96.02	28.49	0.32	-3.06	82.17	0.14
<b>D9</b>	96.70	47.03	0.39	-3.38	81.51	0.18
<b>D12</b>	87.64	17.21	0.30	-3.95	80.56	0.22
<b>D15</b>	87.65	11.88	0.54	-3.95	78.36	0.25
<b>D16</b>	96.42	29.32	0.28	-3.17	81.26	0.14

### 3.6.2. Molecular docking analysis

Molecular docking analysis of the derivatives showing tyrosinase inhibitory activity was performed in order to theoretically describe the difference found in the antityrosinase activity of the compounds and also to inquire the ligands binding modes and possible interactions into the binding pocket of tyrosinase. The enzyme–inhibitor complexes binding affinities are presented in **Table 4**. The lower value indicated the more stable complex formed between the ligand and target enzyme. The most active benzohydrazide derivatives **D5** and **D12**, containing 2-chlorophenyl and 2,3-dihydroxyphenyl groups, respectively, possessed the most negative estimated free energies of binding (-6.91 and -6.66 kcal/mol, respectively), however, their binding modes were completely different. The binding orientations and interactions of **D5** and **D12** with the active site of mushroom tyrosinase are illustrated in **Figure 3a** and **Figure 3b**, respectively. The binding energies of compounds **D7**, **D9**, **D11**, **D15** and **D16** were -5.95, -5.89,

5.77, 6.23 and 5.93 kcal/mol, respectively. The estimated free energies of binding proved that compound **D5** and **D12** made the most stable complex with the target protein. Docking validation was done by extracting the structure of the co-crystallized ligand and re-docking it into the receptor (self-docking). The root mean square deviation (RMSD) between the best pose of co-crystallized ligand docked into the binding site of tyrosinase and the one in the crystal structure was 1.63 Å

**D5** is well accommodated in the binding site of tyrosinase by hydrogen-bond and Pi-H interactions. As it is illustrated in **Figure 3a**, oxygen atoms of carbonyl and 4-methoxy moieties established strong hydrogen bonds with Val283 (distance: 2.03 Å) and Arg268 (distance: 2.03 Å), respectively. Furthermore, 4'-Cl substituent interacted with Cu (distance: 2.67 Å) and 4-chlorophenyl ring involved in a Pi-H interaction with Val283. Compound **D12** accommodated within the active site through three hydrogen bonds (**Figure 3b**). Nitrogen atom of hydrazine group (=N-NH) formed a hydrogen bond interaction with the residue Val283 at a distance of 1.94 Å. The two other hydrogen bond interactions were established between 2'-OH and 3'-OH substitutions and Glu265 residue at distances of 1.71 and 1.97 Å, respectively.

The docking results are in good agreement with the experimental outcomes. These results confirmed that the substitutions on benzylidene moiety had a significant effect in binding orientations of N'-benzylidene-3,4-dimethoxybenzohydrazide within the active site of tyrosinase. Copper atoms and some residues including Val283, Arg268, Gly231, His244, His263, His259 Met280, Glu265 and Phe264 played an influential role in the formation of stable ligand-target complexes.

**Table 4.** Docking results of the presented tyrosinase inhibitors into the tyrosinase binding site.

Compound	$\Delta G$ (kcal/mol)	Ki ( $\mu M$ )	Interactions	Atom of ligand	Amino acid	Distance ( $\text{\AA}$ )
D5	-6.91	8.64	H-bonding	C=O	Val283	2.03
			H-bonding	4-Methoxy	Arg268	2.03
				Cl	Cu	2.67
			Pi-H	4-Cholorophenyl	Val283	
D7	-5.95	43.78	H-bonding	C=O	Val283	1.83
D9	-5.89	47.77	H-bonding	NH of hydrazine (=N-NH)	Gly231	1.83
			H-bonding	N of Hydrazine (=N-NH)	Val283	2.39
			Pi-H	3,4-Dimethoxyphenyl	Val283	
D12	-6.66	18.61	H-bonding	N of hydrazine (=N-NH-)	His244	1.94
			H-bonding	2'-OH	Glu265	1.71
			H-bonding	3'-OH	Glu265	1.95
D15	-6.23	26.98	H-bonding	C=O	Val283	1.79
			H-bonding	2'-OH	Met280	2.03
			Coordinate-bond	4'-OH	Cu	2.56
D16	-5.93	44.99	Pi-Pi	3,4-Dimethoxyphenyl	His244	
			Pi-Pi	4-Acetoxy-3-methoxyphenyl	His259	
			Pi-H	4-Acetoxy-3-methoxyphenyl	Val283	
			Alkyl-Pi	3'-Methoxy	Phe264	
			Alkyl-Pi	4'-Acetoxy	His263	

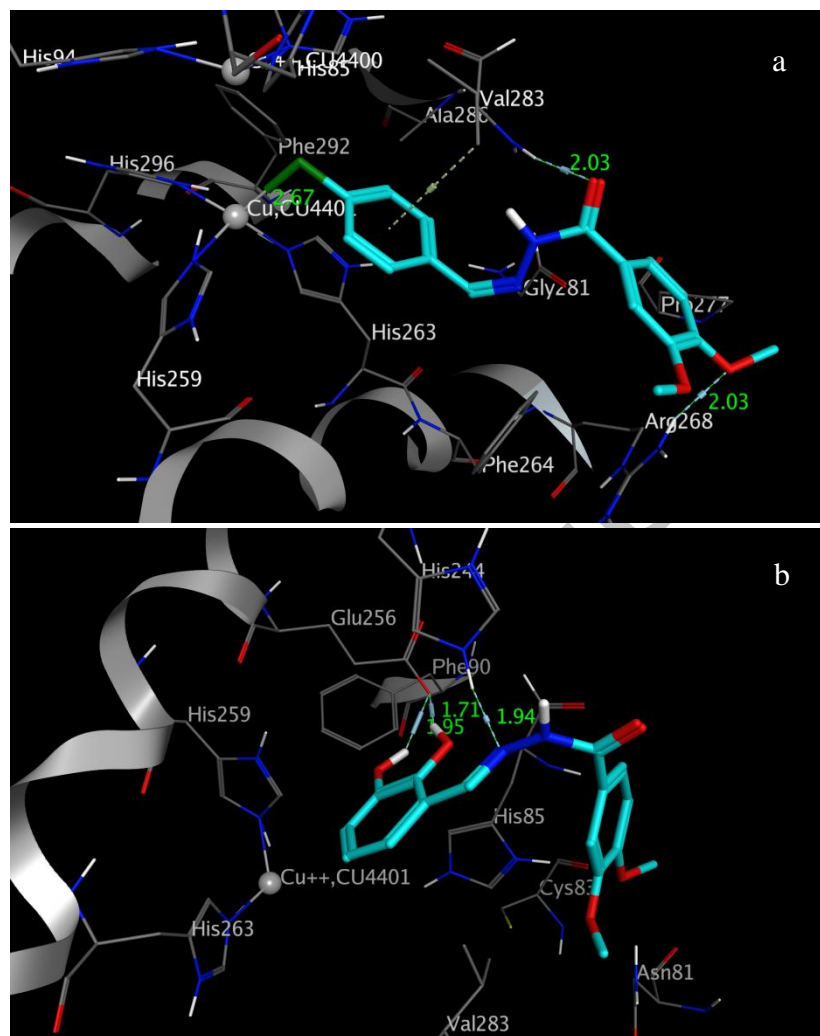


**Figure 3.** The binding orientation of the most active derivatives **D5** (a) and **D12** (b) within the active site of tyrosinase (PDB: 2Y9X). Ligands are shown as cyan sticks while the amino acid residues are displayed as gray sticks.

#### 4. Conclusions

We developed a series of veratric acid derivatives containing benzylidene-hydrazine moieties as novel tyrosinase inhibitors. While, veratric acid and its methyl ester did not show

significant inhibitory effect on tyrosinase, the results showed that some of our target analogues demonstrated remarkable tyrosinase inhibitory activities with  $IC_{50}$  values of micro molar range. Compounds **D5** and **D12** were found to be promising tyrosinase inhibitors with the  $IC_{50}$  values of  $19.72 \pm 1.84$  and  $20.63 \pm 0.79$   $\mu$ M, respectively. The kinetic analysis disclosed a competitive mode of inhibition for **D5**. Docking studies were performed to delineate the binding affinity of the active derivatives in the binding site of tyrosinase. Docking studies showed good correlation with experimental results. Some derivatives also indicated good free radical scavenging activity. **D12** demonstrated the highest activity with  $EC_{50}$  value of  $0.0097 \pm 0.0011$  mM, comparable to that of quercetin. The *in silico* studies further indicated that the active compounds are compliant with most of the rules which lie under drug likeness and pharmacokinetics analysis. It can be concluded that the compounds can serve as structural outlines and promising leads in order to design and develop potential tyrosinase inhibitors.

### Conflicts of interest

The authors confirm that this article content has no conflict of interest.

### Acknowledgments

The authors wish to thank Vice-Chancellor for Research of Shiraz University of Medical Sciences for supporting this study with project No. 97-01-36-18236.

### References

1. Olianias A, Sanjust E, Pellegrini M, Rescigno A. Tyrosinase activity and hemocyanin in the hemolymph of the slipper lobster *Scyllarides latus*. *J Comp Physiol B*. 2005;175:405-11.
2. Sánchez-Ferrer A, Rodríguez-López JN, García-Cánovas F, García-Carmona F. Tyrosinase: a comprehensive review of its mechanism. *Biochimica et Biophysica Acta (BBA)- Protein Structure and Molecular Enzymology*. 1995;1247:1-11.
3. Decker H, Tuczec F. Tyrosinase/catecholoxidase activity of hemocyanins: structural basis and molecular mechanism. *Trends Biochem Sci*. 2000;25:392-7.
4. Kanteev M, Goldfeder M, Fishman A. Structure–function correlations in tyrosinases. *Protein. Science*. 2015;24:1360-9.
5. Hasegawa T. Tyrosinase-expressing neuronal cell line as in vitro model of Parkinson's disease. *Int J Mol Sci*. 2010;11:1082-9.
6. Asanuma M, Miyazaki I, Ogawa N. Dopamine-or L-DOPA-induced neurotoxicity: the role of dopamine quinone formation and tyrosinase in a model of Parkinson's disease. *Neurotox Res*. 2003;5:165-76.
7. Tessari I, Bisaglia M, Valle F, Samorì B, Bergantino E, Mammi S, et al. The Reaction of  $\alpha$ -Synuclein with Tyrosinase possible implications for parkinson disease. *J Biol Chem*. 2008;283:16808-17.
8. McEvily AJ, Iyengar R, Otwell WS. Inhibition of enzymatic browning in foods and beverages. *Crit Rev Food Sci Nutr*. 1992;32:253-73.
9. Chang T-S. An updated review of tyrosinase inhibitors. *Int J Mol Sci*. 2009;10:2440-75.
10. Parvez S, Kang M, Chung HS, Bae H. Naturally occurring tyrosinase inhibitors: mechanism and applications in skin health, cosmetics and agriculture industries. *Phytotherapy*

Research: An International Journal Devoted to Pharmacological and Toxicological Evaluation of Natural Product Derivatives. 2007;21:805-16.

11. Sarkar R, Ranjan R, Garg S, Garg VK, Sonthalia S, Bansal S. Periorbital hyperpigmentation: a comprehensive review. *J Clin Aesthet Dermatol*. 2016;9:49.

12. Zolghadri S, Bahrami A, Hassan Khan MT, Munoz-Munoz J, Garcia-Molina F, Garcia-Canovas F, et al. A comprehensive review on tyrosinase inhibitors. *Enzyme Inhib Med Chem*. 2019;34:279-309.

13. Lee SY, Baek N, Nam T-g. Natural, semisynthetic and synthetic tyrosinase inhibitors. *Enzyme Inhib Med Chem*. 2016;31:1-13.

14. Narasimhan B, Ohlan S, Ohlan R, Judge V, Narang R. Hansch analysis of veratric acid derivatives as antimicrobial agents. *Eur J Med Chem*. 2009;44:689-700.

15. Saravanakumar M, Raja B. Veratric acid, a phenolic acid attenuates blood pressure and oxidative stress in L-NAME induced hypertensive rats. *Eur J Pharmacol*. 2011;671:87-94.

16. Choi W-S, Shin P-G, Lee J-H, Kim G-D. The regulatory effect of veratric acid on NO production in LPS-stimulated RAW264. 7 macrophage cells. *Cell Immunol*. 2012;280:164-70.

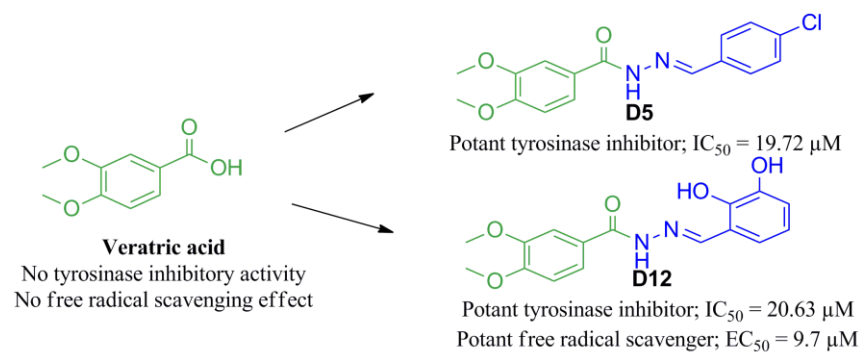
17. Wang Q-b, Sun L-y, Du Y. Veratric acid inhibits LPS-induced IL-6 and IL-8 production in human gingival fibroblasts. *Inflammation*. 2016;39:237-42.

18. Saravanakumar M, Raja B, Manivannan J, Silambarasan T, Prahalathan P, Kumar S, et al. Oral administration of veratric acid, a constituent of vegetables and fruits, prevents cardiovascular remodelling in hypertensive rats: a functional evaluation. *Br J Nutr*. 2015;114:1385-94.

19. Miyazawa M, Oshima T, Koshio K, Itsuzaki Y, Anzai J. Tyrosinase inhibitor from black rice bran. *J Agric Food Chem*. 2003;51:6953-6.

20. Narang R, Narasimhan B, Sharma S. A review on biological activities and chemical synthesis of hydrazide derivatives. *Curr Med Chem.* 2012;19:569-612.
21. Abdel-Aziz M, Abdel-Rahman HM. Synthesis and anti-mycobacterial evaluation of some pyrazine-2-carboxylic acid hydrazide derivatives. *Eur J Med Chem.* 2010;45:3384-8.
22. Gurkok G, Altanlar N, Suzen S. Investigation of antimicrobial activities of indole-3-aldehyde hydrazide/hydrazone derivatives. *Chemotherapy.* 2009;55:15-9.
23. Kajal A, Bala S, Kamboj S, Saini V. Synthesis, characterization, and computational studies on phthalic anhydride-based benzylidene-hydrazide derivatives as novel, potential anti-inflammatory agents. *Med Chem Res.* 2014;23:2676-89.
24. Dimmock JR, Vashishtha SC, Stables JP. Anticonvulsant properties of various acetylhydrazones, oxamoylhydrazones and semicarbazones derived from aromatic and unsaturated carbonyl compounds. *Eur J Med Chem.* 2000;35:241-8.
25. Silva AG, Zapata-Sudo G, Kummerle AE, Fraga CA, Barreiro EJ, Sudo RT. Synthesis and vasodilatory activity of new N-acylhydrazone derivatives, designed as LASSBio-294 analogues. *Bioorg Med Chem.* 2005;13:3431-7.
26. Taha M, Ismail NH, Zaki HM, Wadood A, Imran S, Yamin BM, et al. 3, 4-Dimethoxybenzohydrazide derivatives as antiulcer: Molecular modeling and density functional studies. *Bioorg Chem.* 2017;75:235-41.
27. Deng Y, Kang D, Shi J, Zhou W, Sun A, Ju J, et al. The semi-synthesis, biological evaluation and docking analysis of the oxime, hydrazine and hydrazide derivatives of platensimycin. *MedChemComm.* 2018;9:789-94.

28. Sreenivasulu R, Reddy KT, Sujitha P, Kumar CG, Raju RR. Synthesis, antiproliferative and apoptosis induction potential activities of novel Bis (indolyl) hydrazide-hydrazone derivatives. *Bioorg Med Chem*. 2019.
29. Mahdavi M, Ashtari A, Khoshneviszadeh M, Ranjbar S, Dehghani A, Akbarzadeh T, et al. Synthesis of new benzimidazole-1, 2, 3-triazole hybrids as tyrosinase inhibitors. *Chem Biodivers*. 2018;15:e1800120
30. Ranjbar S, Akbari A, Edraki N, Khoshneviszadeh M, Hemmatian H, Firuzi O, et al. 6-Methoxy-3, 4-dihydronaphthalenone Chalcone-like Derivatives as Potent Tyrosinase Inhibitors and Radical Scavengers. *Lett Drug Des Discov*. 2018;15:1170-9.
31. Tehrani MB, Emani P, Rezaei Z, Khoshneviszadeh M, Ebrahimi M, Edraki N, et al. Phthalimide-1, 2, 3-triazole hybrid compounds as tyrosinase inhibitors; synthesis, biological evaluation and molecular docking analysis. *J Mol Struct*. 2019;1176:86-93.
32. Baek HS, Hong YD, Lee CS, Rho HS, Shin SS, Park Y-H, et al. Adamantyl N-benzylbenzamide: new series of depigmentation agents with tyrosinase inhibitory activity. *Bioorg Med Chem Lett*. 2012;22:2110-3.
33. Yi W, Cao R-H, Chen Z-Y, Yu L, Ma L, Song H-C. Design, synthesis and biological evaluation of hydroxy-or methoxy-substituted phenylmethylenethiosemicarbazones as tyrosinase inhibitors. *Chem Pharm Bull*. 2009;57:1273-7.



ACCEPTED MANUSCRIPT